

## Theoretical studies on two-proton radioactivity

K. P. Santhosh \**School of Pure and Applied Physics, Swami Anandatheertha Campus, Kannur University, Payyanur 670327, Kerala, India*

(Received 19 September 2021; accepted 6 December 2021; published 17 December 2021; corrected 18 October 2022)

The Coulomb and proximity potential model for deformed nuclei (CPPMDN) have been used to compute half-lives of two-proton ( $2p$ ) radioactivity of  ${}^6\text{Be}$ ,  ${}^{12}\text{O}$ ,  ${}^{16}\text{Ne}$ ,  ${}^{19}\text{Mg}$ ,  ${}^{45}\text{Fe}$ ,  ${}^{48}\text{Ni}$ ,  ${}^{54}\text{Zn}$ , and  ${}^{67}\text{Kr}$ , and the values are compared with the experimental data. The predicted half-life values are also compared with six theoretical models and two empirical formulas. The standard deviation is least for the model CPPMDN ( $\sigma = 1.03$ ), compared to other theoretical models and formulas, which indicates that CPPMDN is the apt model for studying  $2p$  radioactivity. I extended the model to predict half-lives of other 15 even- $Z$  nuclei for which  $2p$  radioactivity is energetically possible with released energy,  $Q_{2p} > 0$ , and hope that the predictions may serve as a guide for future experimental investigations. The observed linear nature of the new Geiger-Nuttall plot of  $\log_{10}[T_{1/2}(s)]$  computed using CPPMDN versus  $(Z_d^{0.8} + \ell^{0.25})Q_{2p}^{-1/2}$ , stresses the reliability of the model in predicting  $2p$  radioactivity half-lives.

DOI: [10.1103/PhysRevC.104.064613](https://doi.org/10.1103/PhysRevC.104.064613)

### I. INTRODUCTION

The two-proton ( $2p$ ) radioactivity, the simultaneous emission of the two-proton is a new exotic decay mode from the unbound even- $Z$  nuclei near or beyond the proton drip line. The experimental and theoretical study on  $2p$  radioactivity will provide information on the nuclear structure. The phenomenon was first predicted in the 1960s by Zel'dovich [1] and Goldansky [2,3]. The first experimental evidence of  $2p$  radioactivity was discovered in the decay of  ${}^{45}\text{Fe}$  [4,5], more than four decade after its theoretical prediction. Subsequently, two-proton radioactivity was observed from  ${}^{54}\text{Zn}$  [6],  ${}^{48}\text{Ni}$  [7],  ${}^{19}\text{Mg}$  [8], and  ${}^{67}\text{Kr}$  [9]. The two-proton emission from very short-lived nuclei, e.g., from  ${}^6\text{Be}$  [10],  ${}^{12}\text{O}$  [11],  ${}^{16}\text{Ne}$  [12], and  ${}^{19}\text{Mg}$  [13] were also observed. Furthermore, the  $2p$  radioactivity of the long-lived isomer  ${}^{94}\text{Ag}^m$ , whose parent nucleus has a very large deformation, was observed by Mukha *et al.* in an experiment performed at GSI [14].

A number of theoretical models, the direct decay model [15–20], the model which treats  $2p$  radioactivity as simultaneous or sequential decay [2,21], and the diproton model [22–25] have been proposed. Gonçalves *et al.* [26] treated the  $2p$  emission process as  ${}^2\text{He}$  cluster radioactivity and computed half-lives of  $2p$  emitters using the effective liquid drop model (ELDM) and found an agreement with experimental data. The authors also predicted half-lives of 33 energetically possible  $2p$  emitters whose released energy is  $Q_{2p} > 0$ . Motivated by the work of Gonçalves *et al.* [26] many papers have been published by several authors using different theoretical models [27–32] treating  $2p$  radioactivity as a  ${}^2\text{He}$  cluster decay process. The work of Cui *et al.* [28] using the generalized liquid drop model (GLDM), were

obtained with better half-life values matching with the experimental values. The four-parameter empirical formula (EF) proposed by Sreeja and Balasubramaiam [33] and the two parameter new Geiger-Nuttall law (GNL) proposed by Liu *et al.* [34] are also successful in reproducing two-proton radioactivity.

Grigorenko [35] investigated two-proton radioactivity as a three-body (core +  $p + p$ ) problem based on the hyperspherical harmonics method and Rotureau *et al.* [36] studied two-proton radioactivity in the framework of the shell model embedded in the continuum. In the present paper, two-proton radioactivity is treated as a two-body problem in which the valence protons decay as a cluster and, as a result, the three-body asymptotic behavior is violated, and the detailed information for the configurations of the valence protons are largely lost. It is to be mentioned that Grigorenko [35] and Rotureau *et al.* [36] have shown that both of these effects play a significant role in the  $2p$  decay process.

In the present paper, the model, the Coulomb and proximity potential model for deformed nuclei (CPPMDN) [37], is used to study  $2p$  radioactivity from various nuclei. The predicted half-life values are compared with available experimental data and other theoretical models and empirical formulas. The CPPMDN [38] and its spherical version, the Coulomb and proximity potential model (CPPM) [39], which have been applied successfully for many years to study  $\alpha$  decay and cluster radioactivity [40–43] and is applied to one-proton radioactivity [44,45] studies.

### II. THE MODEL CPPMDN

In the CPPMDN, the sum of the Coulomb potential for deformed nuclei  $V_C(r, \theta)$ , the two-term proximity potential for deformed nuclei  $V_{P2}$ , and centrifugal potential are taken as the

\*drkpsanthosh@gmail.com

interacting potential for the postscission region. It is given by

$$V = V_C(r, \theta) + V_{P2}(r, \theta) + \frac{\hbar^2 \ell(\ell + 1)}{2\mu r^2}, \quad (1)$$

where  $\ell$  represents the angular momentum and  $\mu$  is the reduced mass.

The Coulomb potential for two deformed and oriented nuclei with higher multipole deformations [46,47] is taken from Ref. [48] and is given as

$$V_C(r, \theta) = \frac{Z_1 Z_2 e^2}{r} + 3Z_1 Z_2 e^2 \sum_{\lambda, i=1,2} \frac{1}{2\lambda + 1} \frac{R_{0i}^\lambda}{r^{\lambda+1}} Y_\lambda^{(0)}(\alpha_i) \times \left[ \beta_{\lambda i} + \frac{4}{7} \beta_{\lambda i}^2 Y_\lambda^{(0)}(\alpha_i) \delta_{\lambda,2} \right]. \quad (2)$$

Here  $r = z + C_1 + C_2$ , is the distance between the fragment centers.  $C_1$  and  $C_2$  are the Süssmann central radii of fragments.

$$R_i(\alpha_i) = R_{0i} \left[ 1 + \sum_{\lambda} \beta_{\lambda i} Y_\lambda^{(0)}(\alpha_i) \right], \quad (3)$$

where  $R_{0i} = 1.28A_i^{1/3} - 0.76 + 0.8A_i^{-1/3}$ . Here  $\alpha_i$  is the angle between the radius vector and the symmetry axis of the  $i$ th nuclei, and it is to be noted that the quadrupole interaction term proportional to  $\beta_{21}\beta_{22}$  is neglected because of its short-range character.

The two-term proximity potential for the interaction between a deformed and a spherical nucleus [49] given as

$$V_{P2}(r, \theta) = 2\pi \left[ \frac{R_1(\alpha)R_C}{R_1(\alpha) + R_C + S} \right]^{1/2} \left[ \frac{R_2(\alpha)R_C}{R_2(\alpha) + R_C + S} \right]^{1/2} \times \left[ \left[ \varepsilon_0(S) + \frac{R_1(\alpha) + R_C}{2R_1(\alpha)R_C} \varepsilon_1(S) \right] \times \left[ \varepsilon_0(S) + \frac{R_2(\alpha) + R_C}{2R_2(\alpha)R_C} \varepsilon_1(S) \right] \right]^{1/2}, \quad (4)$$

where  $R_1(\alpha)$  and  $R_2(\alpha)$  are the principal radii of the curvature of the daughter nuclei where the polar angle is  $\alpha$ ,  $R_C$  is the radius of the spherical cluster,  $S$  is the distance between the surfaces along the straight line connecting the fragments, and  $\varepsilon_0(S)$  and  $\varepsilon_1(S)$  are the one-dimensional slab-on-slab function. The relation between  $\alpha$  and  $\theta$  in Eqs. (3) and (4) is given by the equation (see Fig. 5 of Ref. [49]),

$$\frac{\cos(\theta - \alpha)}{R_T(\alpha)} + \frac{\sin(\theta - \alpha)}{R'_T(\alpha)} = \frac{1}{R}, \quad (5)$$

where  $R_T(\alpha)$  is the radius of deformed nuclei in a direction  $\alpha$  from the symmetry axis,  $R'_T(\alpha) = (dR/d\alpha)$  and  $R$  is the distance between the fragment centers,

$$V = a_0(L - L_0)^n \quad (6)$$

is the simple power-law interpolation [50] used for the internal part or the prescission (overlap) region of the barrier. Here  $L = z + 2C_1 + 2C_2$  is the overall separation of the fragments, and  $L_0 = 2C$  is the diameter of the parent nuclei with  $C$  as the Süssmann central radii of the parent nuclei. By equating the

two potentials at the touching point, the value of the constants  $a_0$  and  $n$  can be determined.

The penetrability  $P$  through the barrier is given by

$$P = \exp \left\{ -\frac{2}{\hbar} \int_a^b \sqrt{2\mu(V - Q)} dz \right\}. \quad (7)$$

Here  $\mu$  is the reduced mass. The equation  $V(a) = V(b) = Q$  provides the condition to determine the turning points “ $a$ ” and “ $b$ ,” and  $Q$  is the energy released.

The barrier penetrability  $P$  of a cluster in a deformed nucleus is different in different directions. The averaging of penetrability over different directions is performed using the equation,

$$P = \frac{1}{2} \int_0^\pi P(Q, \theta, \ell) \sin(\theta) d\theta, \quad (8)$$

where  $P(Q, \theta, \ell)$  is the penetrability of a cluster in direction  $\theta$  from the symmetry axis for axially symmetric deformed nuclei.

The decay half-life is given by

$$T_{1/2} = \left( \frac{\ln 2}{\nu P} \right). \quad (9)$$

Here the assault frequency is  $\nu = (2E_v/\hbar)$ . The empirical vibration energy  $E_v$  is given as [51]

$$E_v = \frac{\pi \hbar (2Q/\mu)^{1/2}}{2(C_1 + C_2)}. \quad (10)$$

Here  $Q$  is the released energy,  $\mu$  is the reduced mass, and  $C_1$  and  $C_2$  are the Süssmann central radii of the fragments.

In the case of spherical nuclei, (in CPPM), the interacting barrier is given by

$$V = \frac{Z_1 Z_2 e^2}{r} + V_p(z) + \frac{\hbar^2 \ell(\ell + 1)}{2\mu r^2} \quad \text{for } z > 0 \quad (11)$$

where “ $z$ ” is the distance between the near surfaces of the fragments.  $V_p$  is the proximity potential [52,53] given as

$$V_p(z) = 4\pi\gamma b \left[ \frac{C_1 C_2}{(C_1 + C_2)} \right] \Phi\left(\frac{z}{b}\right), \quad (12)$$

with  $\gamma$  as the nuclear surface tension coefficient and  $\Phi$  as the universal proximity potential [53].

Then the penetrability and half-lives can be determined using Eqs. (7) and (9).

### III. RESULTS AND DISCUSSION

Two-proton ( $2p$ ) radioactivity is energetically possible only if the energy released in the reaction  $Q_{2p}$  is positive and is calculated using the equation,

$$Q_{2p} = \Delta M_p - (\Delta M_{2p} + \Delta M_d). \quad (13)$$

Here  $\Delta M_p$ ,  $\Delta M_{2p}$ , and  $\Delta M_d$  is the mass excess of the parent nuclei,  $2p$  system, and daughter nuclei, respectively, and can be taken from the recent mass tables [54]. The mass excess of the  $2p$  system is equal to twice the mass excess of proton, i.e.,  $\Delta M_{2p} = 2 \times \Delta M_p$  since the  $2p$  system is an unbound system consisting of two protons. In true  $2p$  radioactivity, only

TABLE I. Comparison of predicted half-lives for  $2p$  emission from various nuclei with the experimental data and other theoretical models and/or formulas. The experimental  $Q_{2p}$  values and half-lives are taken from Refs. [28,56].

| Nuclei                  | $Q_{2p}^{\text{expt.}}$ (MeV) | $\log_{10}[T_{1/2}(s)]$  |         |              |              |             |             |             |             |             |            |
|-------------------------|-------------------------------|--------------------------|---------|--------------|--------------|-------------|-------------|-------------|-------------|-------------|------------|
|                         |                               | Expt.                    | Present | GLDM<br>[28] | ELDM<br>[26] | GLM<br>[29] | SEB<br>[30] | SHF<br>[31] | UFM<br>[32] | GNL<br>[34] | EF<br>[33] |
| ${}^6_4\text{Be}$       | 1.371(5)                      | $-20.30^{+0.03}_{-0.03}$ | -21.91  | -19.37       | -19.97       | -19.70      | -19.86      |             | -19.41      | -23.81      | -21.95     |
| ${}^{12}_8\text{O}$     | 1.638(24)                     | $> -20.20$               | -20.90  | -19.17       | -18.27       | -18.04      | -17.70      |             | -18.45      | -20.17      | -18.47     |
|                         | 1.820(120)                    | $-20.94^{+0.43}_{-0.21}$ | -21.22  | -19.46       |              | -18.30      | -18.03      |             | -18.69      | -20.52      | -18.79     |
|                         | 1.790(40)                     | $-21.10^{+0.18}_{-0.13}$ | -21.17  | -19.43       |              | -18.26      | -17.98      |             | -18.65      | -20.46      | -18.74     |
|                         | 1.800(400)                    | $-21.12^{+0.78}_{-0.26}$ | -21.19  | -19.44       |              | -18.27      | -18.00      |             | -18.66      | -20.48      | -18.76     |
| ${}^{16}_{10}\text{Ne}$ | 1.330(80)                     | $-20.64^{+0.30}_{-0.18}$ | -18.01  | -16.45       |              | -16.23      | -15.47      |             | -16.49      | -17.53      | -15.49     |
|                         | 1.400(20)                     | $-20.38^{+0.03}_{-0.03}$ | -18.25  | -16.63       | -16.60       | -16.43      | -15.71      |             | -16.68      | -17.77      | -16.16     |
| ${}^{19}_{12}\text{Mg}$ | 0.750(50)                     | $-11.40^{+0.14}_{-0.20}$ | -11.96  | -11.79       | -11.72       | -11.46      | -10.58      | -11.00      | -11.77      | -12.03      | -10.66     |
| ${}^{45}_{26}\text{Fe}$ | 1.100(100)                    | $-2.40^{+0.26}_{-0.26}$  | -2.76   | -2.23        |              | -2.09       | -2.32       | -2.31       | -1.94       | -2.21       | -1.81      |
|                         | 1.140(50)                     | $-2.07^{+0.24}_{-0.21}$  | -2.36   | -2.71        |              | -2.58       | -2.67       | -2.87       | -2.43       | -2.64       | -1.76      |
|                         | 1.154(16)                     | $-2.55^{+0.13}_{-0.12}$  | -2.53   | -2.87        | -2.43        | -2.74       | -2.78       | -2.88       | -2.60       | -2.79       | -1.81      |
|                         | 1.210(50)                     | $-2.42^{+0.03}_{-0.03}$  | -3.15   | -3.50        |              | -3.37       | -3.24       | -3.53       | -3.23       | -3.35       | -1.66      |
| ${}^{48}_{28}\text{Ni}$ | 1.290(40)                     | $-2.52^{+0.24}_{-0.22}$  | -2.17   | -2.62        |              | -2.59       | -2.55       | -2.23       | -2.29       | -2.59       | -1.61      |
|                         | 1.350(20)                     | $-2.08^{+0.40}_{-0.78}$  | -2.79   | -3.24        |              | -3.21       | -3.00       | -2.27       | -2.91       | -3.13       | -2.13      |
|                         | 1.310(40)                     | $-2.52^{+0.24}_{-0.22}$  | -2.38   | -2.83        | -2.36        |             |             |             | -2.50       |             |            |
| ${}^{54}_{30}\text{Zn}$ | 1.280(210)                    | $-2.76^{+0.15}_{-0.14}$  | -1.45   | -0.87        |              | -0.93       | -1.31       | -1.32       | -0.52       | -1.01       | -0.10      |
|                         | 1.480(20)                     | $-2.43^{+0.20}_{-0.14}$  | -2.59   | -2.95        | -2.52        | -3.01       | -2.81       | -2.08       | -2.61       | -2.81       | -1.83      |
| ${}^{67}_{36}\text{Kr}$ | 1.690(17)                     | $-1.70^{+0.02}_{-0.02}$  | -1.06   | -1.25        | -0.06        | -0.76       | -0.95       | -1.05       | -0.54       | -0.58       | 0.31       |

$2p$  emissions are allowed whereas  $1p$  emissions are forbidden, i.e., in the case of true  $2p$  radioactivity, the energy released  $Q_{2p} > 0$  and  $Q_{1p} < 0$ , where  $Q_{1p}$  is the energy released in  $1p$  radioactivity.

In this paper, first I have calculated the half-lives of  $2p$  radioactivity of  ${}^6\text{Be}$ ,  ${}^{12}\text{O}$ ,  ${}^{16}\text{Ne}$ ,  ${}^{19}\text{Mg}$ ,  ${}^{45}\text{Fe}$ ,  ${}^{48}\text{Ni}$ ,  ${}^{54}\text{Zn}$ , and  ${}^{67}\text{Kr}$  using the CPPMDN, and the predicted half-life values are compared with experimental data and with six theoretical models and two empirical formulas. In the CPPMDN, the external potential is constructed by taking the deformed Coulomb potential, the deformed two-term proximity potential, and the centrifugal potential. The deformed potential is used to simulate the deformation effect, and  $\ell$  orbital in the centrifugal potential is determined by the spin-parity of the parent and daughter nuclei. Here, in the calculation of the half-lives of the  $2p$  emitters, the overlapping effects also are included for which the simple power-law interpolation is used. In the CPPMDN, the effect of quadrupole deformation ( $\beta_2$ ) of the parent and daughter are included. The deformation values are taken from the mass tables of Möller *et al.* [55]. Most of the  $2p$  emitters considered here are far from the  $\beta$ -stability line whose deformation values are not listed in Ref. [55] (such as  ${}^6\text{Be}$ ,  ${}^{12}\text{O}$ ,  ${}^{16}\text{Ne}$ , and  ${}^{19}\text{Mg}$ ), and the calculations are performed treating these nuclei as spherical. The theoretical predictions and their comparison are given in Table I. In this table, the first, second, and third columns give the nuclei which exhibit  $2p$  radioactivity, the experimental  $Q_{2p}$  values, and experimental half-lives, respectively. The experimental data are taken from Refs. [28,56]. Columns 4–12 represent the half-life values predicted by the model CPPMDN with

considering deformation, the GLDM [28], the ELDM [26], the Gamow-like model (GLM) [29], the screened electrostatic barrier (SEB) [30], the two-potential approach with Skyrme Hartree Fock (SHF) [31], the unified fission model (UFM) [32], the new GNL [34], and the EF [33], respectively.

To check the agreement between  $2p$  radioactivity half-lives calculated using the CPPMDN and experimental data, the standard deviation  $\sigma$  is calculated, which is defined by

$$\sigma = \left\{ \frac{1}{n} \sum_{i=1}^n (\log_{10} T_i^{\text{cal.}} - \log_{10} T_i^{\text{expt.}})^2 \right\}^{1/2}. \quad (14)$$

Here  $\log_{10} T_i^{\text{cal.}}$  and  $\log_{10} T_i^{\text{expt.}}$  represent the logarithm of calculated and experimental half-lives for the  $i$ th nucleus. The standard deviation  $\sigma$  for other six theoretical models and two empirical formulas are also computed using Eq. (14). All the computed results are given in Table II. From the table, it is clear that the  $\sigma$  value is least for the model CPPMDN ( $\sigma = 1.03$ ), compared to other theoretical models and/or formulas, which indicate that the CPPMDN is the apt model for studying  $2p$  radioactivity.

In order to illustrate the effect of deformation, the half-lives of nuclei which exhibit  $2p$  radioactivity are computed within the model CPPMDN without considering deformation (spherical case) and with considering deformation are listed in Table III. The predicted values are compared with the experimental half-lives. In Table III, the first and second columns represent the  $2p$  emitters and experimental  $Q_{2p}$  values, respectively. Columns 3 and 4 represent the quadrupole deformation

TABLE II. The standard deviation  $\sigma$  between the experimental data and the predicted half-life values using different theoretical models and/or formulas.

| Model    | Present | GLDM [28] | ELDM [26] | GLM [29] | SEB [30] | SHF [31] | UFM [32] | GNL [34] | EF [33] |
|----------|---------|-----------|-----------|----------|----------|----------|----------|----------|---------|
| $\sigma$ | 1.03    | 1.67      | 1.57      | 2.03     | 2.27     | 2.21     | 1.83     | 1.52     | 2.20    |
| Cases    | 17      | 17        | 7         | 16       | 16       | 10       | 17       | 16       | 16      |

values of the parent and daughter nuclei, respectively, taken from Möller *et al.* [55]. Columns 5–7, respectively, represent the experimental half-lives, the half-lives predicted using the CPPMDN without considering deformation and with considering deformation. From Table III, the decrease in the  $2p$ -decay half-lives with the inclusion of deformation are clearly evident.

The good agreement between computed half-life values with experimental data and with other theoretical predictions, I extended my studies to other 15 even- $Z$  nuclei for which  $2p$  radioactivity is energetically possible with released energy  $Q_{2p} > 0$ . The predicted half-life values using the CPPMDN and their comparison with other theoretical models and formulas are listed in Table IV. In this table the first, second, and third columns represent the nuclei, energy released  $Q_{2p}$ , and angular momentum  $\ell$  carried away by two emitted protons respectively. The  $Q_{2p}$  values and angular momentum  $\ell$  values are taken from Ref. [26]. For nuclei  $^{55}\text{Zn}$  and  $^{64}\text{Se}$ , the  $Q_{2p}$  values are taken from Ref. [28]. Columns 4–11 represent the half-life values predicted by the model CPP-

MDN with including deformation effects, the GLDM [28], the ELDM [26], the GLM [29], the SEB [30], the two-potential approach with SHF [31], the new GNL [34], and the EF [33], respectively. From the table, it is clear that overall the half-life values predicted by the CPPMDN match with other theoretical predictions. The difference (deviation) between the CPPMDN predictions and the GLDM values are very small, but the deviation from the EF are large. To study the effect of deformation, the  $2p$  decay half-lives of 15 even- $Z$  nuclei are calculated using the CPPMDN without and with considering deformation and are listed in Table V. The first, second, and third columns represent the nuclei, energy released  $Q_{2p}$ , and angular momentum  $\ell$  carried away by two emitted protons, respectively. The fourth and fifth columns represent the deformation values of the parent and daughter nuclei taken from Möller *et al.* [55]. The sixth and seventh columns represent the CPPMDN values without considering deformation (spherical case) and with considering deformation, respectively. When the half-life values in these two columns for each nuclei, are compared, it can be seen that

TABLE III. Comparison of predicted half-lives for  $2p$  emission from various nuclei using the CPPMDN without considering deformation and with considering deformation with the experimental data. The experimental  $Q_{2p}$  values and half-lives are taken from Refs. [28,56]. The deformation values are taken from Möller *et al.* [55].

| Nuclei                | $Q_{2p}^{\text{expt.}}$ (MeV) | Deformation $\beta_2$ |          | $\log_{10}[T_{1/2}(s)]$  |                          |                         |
|-----------------------|-------------------------------|-----------------------|----------|--------------------------|--------------------------|-------------------------|
|                       |                               | Parent                | Daughter | Expt.                    | Present                  |                         |
|                       |                               |                       |          |                          | Spherical                | Deformed                |
| $^6\text{Be}$         | 1.371(5)                      |                       |          | $-20.30^{+0.03}_{-0.03}$ | $-21.91^{+0.10}_{-0.10}$ |                         |
| $^{12}_8\text{O}$     | 1.638(24)                     |                       |          | $> -20.20$               | $-20.90^{+0.18}_{-0.17}$ |                         |
|                       | 1.820(120)                    |                       |          | $-20.94^{+0.43}_{-0.21}$ | $-21.22^{+0.48}_{-0.43}$ |                         |
|                       | 1.790(40)                     |                       |          | $-21.10^{+0.18}_{-0.13}$ | $-21.17^{+0.18}_{-0.18}$ |                         |
|                       | 1.800(400)                    |                       |          | $-21.12^{+0.78}_{-0.26}$ | $-21.19^{+0.38}_{-0.38}$ |                         |
|                       | 1.330(80)                     |                       |          | $-20.64^{+0.30}_{-0.18}$ | $-18.01^{+0.10}_{-0.10}$ |                         |
| $^{16}_{10}\text{Ne}$ | 1.400(20)                     |                       |          | $-20.38^{+0.03}_{-0.03}$ | $-18.25^{+0.08}_{-0.07}$ |                         |
|                       | 0.750(50)                     |                       |          | $-11.40^{+0.14}_{-0.20}$ | $-11.96^{+0.14}_{-0.15}$ |                         |
| $^{45}_{26}\text{Fe}$ | 1.100(100)                    | 0.086                 | 0.086    | $-2.40^{+0.26}_{-0.26}$  | $-2.45^{+0.20}_{-0.30}$  | $-2.76^{+0.20}_{-0.30}$ |
|                       | 1.140(50)                     |                       |          | $-2.07^{+0.24}_{-0.21}$  | $-2.05^{+0.59}_{-0.63}$  | $-2.36^{+0.59}_{-0.63}$ |
|                       | 1.154(16)                     |                       |          | $-2.55^{+0.13}_{-0.12}$  | $-2.34^{+0.19}_{-0.19}$  | $-2.53^{+0.19}_{-0.19}$ |
|                       | 1.210(50)                     |                       |          | $-2.42^{+0.03}_{-0.03}$  | $-2.84^{+0.57}_{-0.55}$  | $-3.15^{+0.57}_{-0.55}$ |
| $^{48}_{28}\text{Ni}$ | 1.290(40)                     | 0.000                 | 0.001    | $-2.52^{+0.24}_{-0.22}$  | $-2.15^{+0.43}_{-0.45}$  | $-2.17^{+0.43}_{-0.45}$ |
|                       | 1.350(20)                     |                       |          | $-2.08^{+0.40}_{-0.78}$  | $-2.78^{+0.20}_{-0.21}$  | $-2.79^{+0.20}_{-0.21}$ |
|                       | 1.310(40)                     |                       |          | $-2.52^{+0.24}_{-0.22}$  | $-2.37^{+0.42}_{-0.45}$  | $-2.38^{+0.42}_{-0.45}$ |
| $^{54}_{30}\text{Zn}$ | 1.280(210)                    | 0.171                 | 0.011    | $-2.76^{+0.15}_{-0.14}$  | $-1.36^{+0.07}_{-0.07}$  | $-1.45^{+0.07}_{-0.07}$ |
|                       | 1.480(20)                     |                       |          | $-2.43^{+0.20}_{-0.14}$  | $-2.51^{+0.19}_{-0.19}$  | $-2.59^{+0.19}_{-0.19}$ |
| $^{67}_{36}\text{Kr}$ | 1.690(17)                     | -0.275                | 0.208    | $-1.70^{+0.02}_{-0.02}$  | $-0.23^{+0.16}_{-0.16}$  | $-1.06^{+0.16}_{-0.16}$ |

TABLE IV. Comparison of our predicted half-lives for various nuclei whose  $2p$  radioactivity are energetically possible with other theoretical models and/or formulas. The released energy  $Q_{2p}$  and angular momentum  $\ell$  are taken from Ref. [26].

| Nuclei                | $Q_{2p}$ (MeV) | $\ell$ | $\log_{10}[T_{1/2}(s)]$ |           |           |          |          |          |          |         |
|-----------------------|----------------|--------|-------------------------|-----------|-----------|----------|----------|----------|----------|---------|
|                       |                |        | Present                 | GLDM [28] | ELDM [26] | GLM [29] | SEB [30] | SHF [31] | GNL [34] | EF [33] |
| $^{16}_{10}\text{Ne}$ | 1.401          | 0      | -17.00                  |           | -16.60    |          |          |          |          | -16.16  |
| $^{19}_{12}\text{Mg}$ | 0.75           | 0      | -11.99                  |           | -11.72    |          |          |          |          | -10.66  |
| $^{22}_{14}\text{Si}$ | 1.283          | 0      | -13.70                  | -13.30    | -13.32    | -13.25   | -12.17   | -11.78   | -13.74   | -12.30  |
| $^{26}_{16}\text{S}$  | 1.755          | 0      | -14.40                  | -14.59    | -13.86    | -13.92   | -12.82   | -12.93   | -14.16   | -12.71  |
| $^{30}_{18}\text{Ar}$ | 2.28           | 0      | -14.99                  |           | -14.32    |          |          |          |          | -13.00  |
| $^{34}_{20}\text{Ca}$ | 1.474          | 0      | -10.44                  | -10.71    | -9.92     | -10.10   | -8.99    | -9.51    | -9.93    | -8.65   |
| $^{38}_{22}\text{Ti}$ | 2.743          | 0      | -14.35                  | -14.27    | -13.56    | -13.84   | -12.70   | -11.77   | -13.35   | -11.93  |
| $^{39}_{22}\text{Ti}$ | 0.758          | 0      | -1.23                   | -1.34     | -0.81     | -0.91    | -1.91    | -1.62    | -1.19    | -0.28   |
| $^{42}_{24}\text{Cr}$ | 1.002          | 0      | -2.86                   | -2.88     | -2.43     | -2.65    | -2.87    | -2.83    | -2.76    | -1.78   |
| $^{49}_{28}\text{Ni}$ | 0.492          | 0      | 14.24                   | 14.46     | 14.64     | 14.54    |          | 11.05    | 12.43    | 12.78   |
| $^{55}_{30}\text{Zn}$ | 0.48           | 0      | 17.66                   | 17.94     |           |          |          |          |          |         |
| $^{58}_{32}\text{Ge}$ | 3.732          | 0      | -12.73                  | -13.10    | -11.74    | -12.32   | -11.10   | -11.06   | -10.85   | -9.53   |
| $^{59}_{32}\text{Ge}$ | 2.102          | 0      | -6.99                   | -6.97     | -5.71     | -6.31    | -5.41    | -5.88    | -5.54    | -4.44   |
| $^{60}_{32}\text{Ge}$ | 0.631          | 0      | 14.00                   | 13.55     | 14.62     | 14.24    |          | 12.09    | 12.04    | 12.40   |
| $^{64}_{34}\text{Se}$ | 0.46           | 0      | 25.03                   | 24.44     |           |          |          |          |          |         |

half-life values are found decreasing with the inclusion of deformation.

When the CPPMDN predictions on  $2p$ -decay half-lives without considering deformation and the predictions with considering deformation are compared (given in Tables III and V), it can be seen that half-life values decrease with the in-

clusion of deformation. The inclusion of deformation reduces the height and width of the barrier, and as a result, penetrability increases, and half-life values decrease. In Table III, the parent nuclei  $^{45}\text{Fe}$  ( $\beta_2 = 0.086$ ),  $^{54}\text{Zn}$  ( $\beta_2 = 0.071$ ), and their daughter nuclei  $^{43}\text{Cr}$  ( $\beta_2 = 0.086$ ),  $^{52}\text{Ni}$  ( $\beta_2 = 0.011$ ) are prolate deformed, the nuclei  $^{48}\text{Ni}$  ( $\beta_2 = 0.000$ ) are spherical whereas their daughter nuclei  $^{46}\text{Fe}$  ( $\beta_2 = 0.001$ ) are slightly

TABLE V. Comparison of the predicted half-lives for various nuclei using the CPPMDN without considering deformation and with considering deformation. The released energy  $Q_{2p}$  and angular momentum  $\ell$  are taken from Ref. [26]. The deformation values are taken from Möller *et al.* [55].

| Nuclei                | $Q_{2p}$ (MeV) | $\ell$ | $\log_{10}[T_{1/2}(s)]$ |          |           |          |
|-----------------------|----------------|--------|-------------------------|----------|-----------|----------|
|                       |                |        | Deformation, $\beta_2$  |          | Present   |          |
|                       |                |        | Parent                  | Daughter | Spherical | Deformed |
| $^{16}_{10}\text{Ne}$ | 1.401          | 0      |                         |          | -17.00    |          |
| $^{19}_{12}\text{Mg}$ | 0.75           | 0      |                         |          | -11.99    |          |
| $^{22}_{14}\text{Si}$ | 1.283          | 0      | 0.001                   | 0.122    | -13.52    | -13.70   |
| $^{26}_{16}\text{S}$  | 1.755          | 0      | 0.126                   |          | -14.36    | -14.40   |
| $^{30}_{18}\text{Ar}$ | 2.28           | 0      | -0.280                  | 0.321    | -14.66    | -14.99   |
| $^{34}_{20}\text{Ca}$ | 1.474          | 0      | 0.000                   | -0.281   | -9.89     | -10.44   |
| $^{38}_{22}\text{Ti}$ | 2.743          | 0      | 0.118                   | 0.000    | -14.30    | -14.35   |
| $^{39}_{22}\text{Ti}$ | 0.758          | 0      | 0.107                   | -0.021   | -1.08     | -1.23    |
| $^{42}_{24}\text{Cr}$ | 1.002          | 0      | 0.118                   | -0.031   | -2.79     | -2.86    |
| $^{49}_{28}\text{Ni}$ | 0.492          | 0      | -0.042                  | 0.065    | 14.37     | 14.24    |
| $^{55}_{30}\text{Zn}$ | 0.48           | 0      | 0.172                   | -0.021   | 17.70     | 17.66    |
| $^{58}_{32}\text{Ge}$ | 3.732          | 0      | 0.173                   | 0.139    | -12.41    | -12.73   |
| $^{59}_{32}\text{Ge}$ | 2.102          | 0      | 0.151                   | 0.096    | -6.63     | -6.99    |
| $^{60}_{32}\text{Ge}$ | 0.631          | 0      | 0.075                   | 0.000    | 14.04     | 14.00    |
| $^{64}_{34}\text{Se}$ | 0.46           | 0      | 0.196                   | 0.184    | 25.78     | 25.03    |



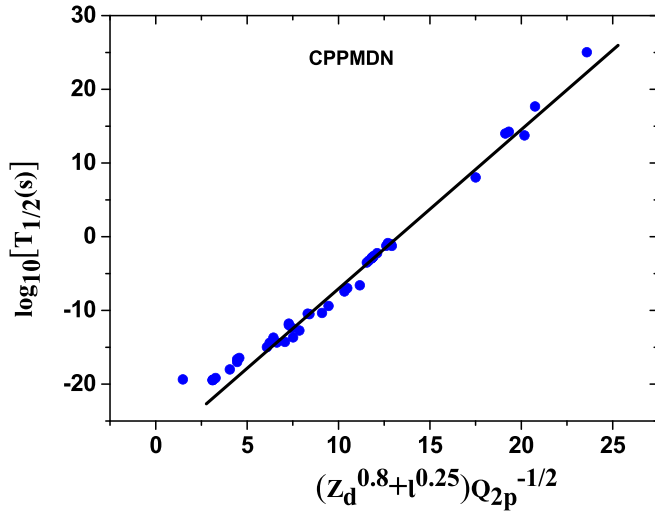


FIG. 1. The plot connecting predicted  $\log_{10}[T_{1/2}(s)]$  versus  $(Z_d^{0.8} + \ell^{0.25})Q_{2p}^{-1/2}$ , the new Geiger-Nuttall law for  $2p$  radioactivity.

prolate.  $^{67}\text{Kr}$  ( $\beta_2 = -0.275$ ) is an oblate-deformed nucleus, and its daughter  $^{65}\text{Se}$  ( $\beta_2 = 0.208$ ) is a prolate-deformed nucleus. In the  $2p$  decay of these parent nuclei, the half-life values are found to decrease with the inclusion of deformation. In the case of  $^{67}\text{Kr}$ , the half-life  $T_{1/2} = 0.589$  s (without deformation) reduces to  $T_{1/2} = 0.087$  s (with deformation). It has been shown by Wang and Nazarewicz [57] that the lifetime of  $^{67}\text{Kr}$  dramatically reduces as the deformation and structure change. In Table V, the deformation value of  $^{24}\text{Si}$ , the daughter nuclei of  $^{26}\text{S}$  (prolate deformed), is not available in the table of Möller *et al.* [55], so this nuclei is treated as spherical. In Table V, it is to be noted that the nuclei  $^{39}\text{Ti}$ ,  $^{42}\text{Cr}$ , and  $^{55}\text{Zn}$  are prolate and their daughters are oblate; the nuclei  $^{30}\text{Ar}$  and  $^{49}\text{Ni}$  are oblate and their daughters are prolate; the nuclei  $^{38}\text{Ti}$  and  $^{60}\text{Ge}$  are prolate and their daughters are spherical; the nuclei  $^{34}\text{Ca}$  is spherical and its daughter is oblate; and the deformation of the rest of parent nuclei and their daughters are both prolate. From Table V, it evident

that  $2p$ -decay half-life values decrease with the inclusion of deformation, even though in most of the cases, parent and daughter nuclei have very different deformations.

The new Geiger-Nuttall law, the relation connecting  $\log_{10}[T_{1/2}(s)]$  and  $(Z_d^{0.8} + \ell^{0.25})Q_{2p}^{-1/2}$  for  $2p$  radioactivity was first introduced by Liu *et al.* [34] and the authors obtained a linear plot with slope = 2.023 and intercept = -26.832. Recently, Zou *et al.* [30] reported that their predicted  $\log_{10}[T_{1/2}(s)]$  values of  $2p$  radioactivity computed with a SEB also showed a linear relation with  $(Z_d^{0.8} + \ell^{0.25})Q_{2p}^{-1/2}$ . Very recently, Pan *et al.* [31] reported that their predicted  $\log_{10}[T_{1/2}(s)]$  values based on the two-potential approach with SHF obey the new Geiger-Nuttall law for  $2p$  radioactivity and showed that the half-life prediction by the models GLDM, ELDM, and GLM also exhibit a similar linear relationship. Figure 1 represents the new Geiger-Nuttall plot of  $\log_{10}[T_{1/2}(s)]$  computed using the CPPMDN versus  $(Z_d^{0.8} + \ell^{0.25})Q_{2p}^{-1/2}$ , the linear nature of the plot stress the reliability of the present model in predicting  $2p$  radioactivity half-lives.

#### IV. SUMMARY

The  $2p$  radioactivity half-lives of  $^6\text{Be}$ ,  $^{12}\text{O}$ ,  $^{16}\text{Ne}$ ,  $^{19}\text{Mg}$ ,  $^{45}\text{Fe}$ ,  $^{48}\text{Ni}$ ,  $^{54}\text{Zn}$ , and  $^{67}\text{Kr}$  are computed using the model CPPMDN, and the predicted values are compared with experimental data and with other theoretical predictions. The obtained standard deviation is least for the CPPMDN ( $\sigma = 1.03$ ), compared to other theoretical models and formulas, which indicate that the CPPMDN can be used for studying  $2p$  radioactivity. I extended my paper to predict half-lives of other 15 even- $Z$  nuclei for which  $2p$  radioactivity is energetically possible with released energy  $Q_{2p} > 0$  and hope that the predictions may serve as a guide for future experimental investigations. The new Geiger-Nuttall plot of  $\log_{10}[T_{1/2}(s)]$  versus  $(Z_d^{0.8} + \ell^{0.25})Q_{2p}^{-1/2}$  is studied, and the linear nature of the plot stress the reliability of the model CPPMDN in predicting  $2p$  radioactivity half-lives.

- [1] Y. B. Zel'dovich, Sov. Phys. JETP **11**, 812 (1960).
- [2] V. I. Goldansky, Nucl. Phys. **19**, 482 (1960).
- [3] V. I. Goldansky, Nucl. Phys. **27**, 648 (1961).
- [4] J. Giovannazzo, B. Blank, M. Chartier, S. Czajkowski, A. Fleury, M. J. Lopez Jimenez, M. S. Pravikoff, J.-C. Thomas, F. de Oliveira Santos, M. Lewitowicz, V. Maslov, M. Stanoiu, R. Grzywacz, M. Pfützner, C. Borcea, and B. A. Brown, Phys. Rev. Lett. **89**, 102501 (2002).
- [5] M. Pfützner, E. Badura, B. Blank, C. Bingham, M. Chartier, H. Geissel, J. Giovannazzo, L. V. Grigorenko, R. Grzywacz, and M. Hellström, Eur. Phys. J. A **14**, 279 (2002).
- [6] B. Blank, A. Bey, G. Canchel, C. Dossat, A. Fleury, J. Giovannazzo, I. Matea, N. Adimi, F. De Oliveira, I. Stefan, G. Georgiev, S. Grévy, J. C. Thomas, C. Borcea, D. Cortina, M. Caamano, M. Stanoiu, F. Aksouh, B. A. Brown, F. C. Barker, and W. A. Richter, Phys. Rev. Lett. **94**, 232501 (2005).
- [7] C. Dossat, A. Bey, B. Blank, G. Canchel, A. Fleury, J. Giovannazzo, I. Matea, F. de Oliveira Santos, G. Georgiev,

- S. Grévy, I. Stefan, J. C. Thomas, N. Adimi, C. Borcea, D. Cortina Gil, M. Caamano, M. Stanoiu, F. Aksouh, B. A. Brown, and L. V. Grigorenko, Phys. Rev. C **72**, 054315 (2005).
- [8] I. Mukha, K. Sümmerner, L. Acosta, M. A. G. Alvarez, E. Casarejos, A. Chatillon, D. Cortina-Gil, J. Espino, A. Fomichev, J. E. García-Ramos, H. Geissel, J. Gómez-Camacho, L. Grigorenko, J. Hoffmann, O. Kiselev, A. Korshennikov, N. Kurz, Yu. Litvinov, I. Martel, C. Nociforo, W. Ott, M. Pfützner, C. Rodríguez-Tajes, E. Roeckl, M. Stanoiu, H. Weick, and P. J. Woods, Phys. Rev. Lett. **99**, 182501 (2007).
- [9] T. Goigoux, P. Ascher, B. Blank, M. Gerbaux, J. Giovannazzo, S. Grévy, T. Kurtukian Nieto, C. Magron, P. Doornenbal, G. G. Kiss *et al.*, Phys. Rev. Lett. **117**, 162501 (2016).
- [10] O. V. Bochkarev, A. A. Korshennikov, E. A. Kuz'min, I. G. Mukha, L. V. Chulkov, and G. B. Yan'kov, Sov. J. Nucl. Phys. **49**, 941 (1989).
- [11] R. A. Kryger, A. Azhari, M. Hellström, J. H. Kelley, T. Kubo, R. Pfaff, E. Ramakrishnan, B. M. Sherrill, M. Thoennessen,

- S. Yokoyama, R. J. Charity, J. Dempsey, A. Kirov, N. Robertson, D. G. Sarantites, L. G. Sobotka, and J. A. Winger, *Phys. Rev. Lett.* **74**, 860 (1995).
- [12] G. J. KeKelis, M. S. Zisman, D. K. Scott, R. Jahn, D. J. Vieira, J. Cerny, and F. Ajzenberg-Selove, *Phys. Rev. C* **17**, 1929 (1978).
- [13] I. Mukha, L. Grigorenko, K. Sümmerer, L. Acosta, M. A. G. Alvarez, E. Casarejos, A. Chatillon, D. Cortina-Gil, J. M. Espino, A. Fomichev, J. E. García-Ramos, H. Geissel, J. Gómez-Camacho, J. Hofmann, O. Kiselev, A. Korshennikov, N. Kurz, Yu. Litvinov, I. Martel, C. Nociforo, W. Ott, M. Pfützner, C. Rodríguez-Tajes, E. Roeckl, M. Stanoiu, H. Weick, and P. J. Woods, *Phys. Rev. C* **77**, 061303(R) (2008).
- [14] I. Mukha, E. Roeckl, L. Batist, A. Blazhev, J. Döring, H. Grawe, L. Grigorenko, M. Huyse, Z. Janas, R. Kirchner, M. La Commara, C. Mazzocchi, S. L. Tabor, and P. V. Duppen, *Nature (London)* **439**, 298 (2006).
- [15] L. V. Grigorenko and M. V. Zhukov, *Phys. Rev. C* **76**, 014009 (2007).
- [16] V. Galitsky and V. Chel'tsov, *Nucl. Phys.* **56**, 86 (1964).
- [17] A. M. Lane and R. G. Thomas, *Rev. Mod. Phys.* **30**, 257 (1958).
- [18] K. Miernik, W. Dominik, Z. Janas, M. Pfützner, L. Grigorenko, C. R. Bingham, H. Czyrkowski, M. Ćwiok, I. G. Darby, R. Dąbrowski, T. Ginter, R. Grzywacz, M. Karny, A. Korgul, W. Kuśmierz, S. N. Liddick, M. Rajabali, K. Rykaczewski, and A. Stolz, *Phys. Rev. Lett.* **99**, 192501 (2007).
- [19] E. Olsen, M. Pfützner, N. Birge, M. Brown, W. Nazarewicz, and A. Perhac, *Phys. Rev. Lett.* **110**, 222501 (2013).
- [20] E. Olsen, M. Pfützner, N. Birge, M. Brown, W. Nazarewicz, and A. Perhac, *Phys. Rev. Lett.* **111**, 139903(E) (2013).
- [21] R. Álvarez-Rodríguez, H. O. U. Fynbo, A. S. Jensen, and E. Garrido, *Phys. Rev. Lett.* **100**, 192501 (2008).
- [22] V. I. Goldansky, *J. Exp. Theor. Phys.* **12**, 348 (1961).
- [23] F. C. Barker, *Phys. Rev. C* **63**, 047303 (2001).
- [24] B. A. Brown, *Phys. Rev. C* **43**, R1513(R) (1991).
- [25] W. Nazarewicz, J. Dobaczewski, T. R. Werner, J. A. Maruhn, P.-G. Reinhard, K. Rutz, C. R. Chinn, A. S. Umar, and M. R. Strayer, *Phys. Rev. C* **53**, 740 (1996).
- [26] M. Gonçalves, N. Teruyab, O. A. P. Tavares, and S. B. Duarte, *Phys. Lett. B* **774**, 14 (2017).
- [27] Y. Wang, J. Cui, Y. Gao, and J. Gu, *Commun. Theor. Phys.* **73**, 075301 (2021).
- [28] J. P. Cui, Y. H. Gao, Y. Z. Wang, and J. Z. Gu, *Phys. Rev. C* **101**, 014301 (2020).
- [29] H.-M. Liu, X. Pan, Y.-T. Zou, J.-L. Chen, J.-H. Cheng, B. He, and X.-H. Li, *Chin. Phys. C* **45**, 044110 (2021).
- [30] You-Tian Zou, Xiao Pan, Xiao-Hua Li, Hong-Ming Liu, Xi-Jun Wu, and Biao He, *Chin. Phys. C* **45**, 104101 (2021).
- [31] Xiao Pan, You-Tian Zou, Hong-Ming Liu, Biao He, Xiao-Hua Li, Xi-Jun Wu, and Zhen Zhang, *Chin. Phys. C* **45**, 124104 (2021).
- [32] F. Xing, J. Cui, Y. Wang, and J. Gu, *Chin. Phys. C* **45**, 124105 (2021).
- [33] I. Sreeja and M. Balasubramaniam, *Eur. Phys. J. A* **55**, 33 (2019).
- [34] H.-M. Liu, Y.-T. Zou, X. Pan, J.-L. Chen, B. He, and X.-H. Li, *Chin. Phys. C* **45**, 024108 (2021).
- [35] L. V. Grigorenko, *Phys. Part. Nucl.* **40**, 674 (2009).
- [36] J. Rotureau, J. Okołowicz, and M. Płoszajczak, *Nucl. Phys. A* **767**, 13 (2006).
- [37] K. P. Santhosh, J. G. Joseph, and S. Sahadevan, *Phys. Rev. C* **82**, 064605 (2010).
- [38] K. P. Santhosh, S. Sabina, and J. G. Joseph, *Nucl. Phys. A* **850**, 34 (2011).
- [39] K. P. Santhosh and A. Joseph, *Pramana* **58**, 611 (2002).
- [40] K. P. Santhosh, I. Sukumaran, and B. Priyanka, *Nucl. Phys. A* **935**, 28 (2015).
- [41] K. P. Santhosh and Indu Sukumaran, *Braz. J. Phys.* **46**, 754 (2016).
- [42] K. P. Santhosh and Indu Sukumaran, *Can. J. Phys.* **95**, 31 (2016).
- [43] K. P. Santhosh, B. Priyanka, and C. Nitya, *Nucl. Phys. A* **955**, 156 (2016).
- [44] K. P. Santhosh and I. Sukumaran, *Phys. Rev. C* **96**, 034619 (2017).
- [45] K. P. Santhosh and I. Sukumaran, *Eur. Phys. J. A* **54**, 102 (2018).
- [46] N. Malhotra and R. K. Gupta, *Phys. Rev. C* **31**, 1179 (1985).
- [47] R. K. Gupta, M. Balasubramaniam, R. Kumar, N. Singh, M. Manhas, and W. Greiner, *J. Phys. G: Nucl. Part. Phys.* **31**, 631 (2005).
- [48] C. Y. Wong, *Phys. Rev. Lett.* **31**, 766 (1973).
- [49] A. J. Baltz and B. F. Bayman, *Phys. Rev. C* **26**, 1969 (1982).
- [50] Y. J. Shi and W. J. Swiatecki, *Nucl. Phys. A* **464**, 205 (1987).
- [51] H. G. de Carvalho, J. B. Martins, and O. A. P. Tavares, *Phys. Rev. C* **34**, 2261 (1986).
- [52] J. Blocki, J. Randrup, W. J. Swiatecki, and C. F. Tsang, *Ann. Phys. (NY)* **105**, 427 (1977).
- [53] J. Blocki and W. J. Swiatecki, *Ann. Phys. (NY)* **132**, 53 (1981).
- [54] F. G. Kondev, M. Wang, W. J. Huang, S. Naimi, and G. Audi, *Chin. Phys. C* **45**, 030001 (2021).
- [55] P. Möller, A. J. Sierk, T. Ichikawa, and H. Sagawa, *At. Data Nucl. Data Tables* **109**, 1 (2016).
- [56] J. P. Cui, Y. H. Gao, Y. Z. Wang, and J. Z. Gu, *Phys. Rev. C* **104**, 029902(E) (2021).
- [57] S. M. Wang and W. Nazarewicz, *Phys. Rev. Lett.* **120**, 212502 (2018).

*Correction:* A term appearing in the last sentence of the abstract was missing a plus sign and has been fixed. The error also occurred in Figure 1 and its caption as well as in the last paragraph of Sec. III and the first paragraph of Sec. IV. A typographical error in an author name in Ref. [5] has also been fixed.